



Thermal Properties of Acetylated Betung Bamboo (*Dendrocalamus asper*) Pulp–Polypropylene Biocomposites

Wida Banar Kusumaningrum ^{a,*}, Sukma Surya Kusumah ^a, Ismadi ^a, Rochmadi ^b, Subyakto ^a

^a Research Center for Biomass and Bioproduct, National Research and Innovation Agency, Cibinong Bogor, 16911, Indonesia

^b Department of Chemical Engineering, Universitas Gadjah Mada, Jl Grafika No. 2, Yogyakarta, Indonesia

* Corresponding author: wida002@brin.go.id

<https://doi.org/10.14710/jksa.26.3.91-100>

Article Info

Article history:

Received: 26th January 2023

Revised: 08th April 2023

Accepted: 10th May 2023

Online: 31st May 2023

Keywords:

Acetylation; Betung bamboo (*D. asper*); Thermal analysis; Pulp; Polypropylene

Abstract

Thermal properties are important factor in determining the proper manufacturing, processing, and storing of biocomposites. This research investigated the acetylation modification and fiber composition on the thermal properties of polypropylene (PP) biocomposites. The acetylation was done using acetic anhydride in 10-fold of dried pulp and 2% (w/v) of sulfuric acid, which processes at 60°C for 2 h. The biocomposite was manufactured by hot pressing at 180°C for 2 minutes. The fiber contents of the acetylated bamboo pulp used were 10% and 20% according to PP weight. The influence of bamboo pulp's acetylation and fiber content on the biocomposite's thermal properties was investigated using a differential scanning calorimeter (DSC) and thermogravimetric analyzer (TGA). The rate of crystallization growth of the 20% of acetylated bamboo pulp-PP biocomposites was faster up to 4.5-fold than pure PP composite. In addition, its acetylated bamboo pulp-PP had higher onset and maximum decomposition temperature than its untreated fiber-PP biocomposites but lower than PP. According to the result, the role of acetylated Betung bamboo fiber is as a nucleating agent in the PP matrix and moderately improving the maximum thermal decomposition of biocomposites for fiber addition by up to 20%.

1. Introduction

Polypropylene (PP) is a polymorphic polymer commonly used for various applications, especially high-durability materials such as automotive body parts, electronic devices, and consumer goods. It remains dominant in the polymer industry due to having excellent properties such as low density, good thermal stability, good chemical inertness, good mechanical properties, and versatile fabrication and product [1]. PP is a non-biodegradable polymer, encouraging modification to support the green movement concepts. Reinforcing with biodegradable substances like natural fiber is one of the accessible technics. One promising source of natural fibers is Betung bamboo (*D. asper*), which is abundantly available in Indonesia. Its fibers, mainly composed of 78.4 and 28.2% holocellulose and lignin, respectively [2], achieve 89.95% and 4.56% of holocellulose and lignin after the pulping process [3].

The mixing process of PP and natural fibers is challenging because polarity differences lead to weak nucleating ability and interfacial adhesion. Moreover, nuclei formation in pure PP is difficult and mainly a homogeneous nucleation due to a slow nucleation rate which affects for molding process [4]. The presence of fibers is expected to facilitate the nucleating ability of PP. However, modifications are carried out to promote compatibility between natural fibers and PP. Potential chemical modifications are performed, such as alkylation, acetylation, silylation, and benzylation [5, 6, 7, 8]. Acetylated sisal fiber was more thermally stable with a maximum degradation temperature of about 361.5°C than alkalization and silylation at 360.75°C and 357.38°C, respectively, and had low weight loss below 100°C which contributes to hydrophobicity characteristic [5]. Acetylation modification in the sponge-gourd fibers resulted in a rougher surface and more thermally stable with a decomposition temperature achieved 341.8°C

compared to alkylation and benzoylation at 309°C and 311°C, respectively [6]. Activation energy to decompose the acetylated bamboo fiber was about 182–201 kJ/mol higher than untreated fiber, corresponding to higher thermal stability [9]. The initial decomposition of acetylated micro fibrillated cellulose was higher than silylated fiber [10]. Acetylation also reduced the polarity of fibers due to hydroxyl group substitution onto acetyl groups, which results in more hydrophobic fibers that enhance the interfacial bonding. At the same time, alkalization only removed the waxy substances in the fiber surface, resulting in a rough surface [7]. Thus, acetylation is preferable, considering polarity enhancement and wide surface area.

Some studies have investigated the effect of acetylated fiber on the PP matrix. Isothermal crystallization, ranging from 122 to 130°C, of acetylated bamboo-PP biocomposites informed that crystallization behavior is affected by crystallinity temperature (T_c), which is more shift for high T_c [11]. Further, Jhu *et al.* [11] reported the appearance of a transcrystallization layer along the acetylated fibers indicating heterogeneous nucleation. The maximum decomposition temperature of acetylated alfa fiber-PP biocomposites increased by about 11°C by 20% of fiber loading than pure PP [12]. Another work from Hamour *et al.* [13] reported about maximum degradation rate of acetylated alfa fiber-PP biocomposites indicating thermal stability improvement. The higher crystallinity degree and T_c suggested the nucleating ability of acetylated alfa-fiber on the PP matrix. Zaman and Khan [7] had a similar result: acetylated banana fiber acts as a nucleating agent on the PP matrix performed by T_c value improvement of about 9°C and crystallization degree of about 9%. Modification by acetylation enables good interfacial adhesion on PP, then promotes nucleating ability and thermal stability performance.

For polymorphic polymers and thermoplastics such as PP, it is beneficial to perform thermal analysis to determine production, handling, and storage processes. The thermal analysis provides information about process conditions, including crystallization temperature and time, for the best molding process to make a certain product. It also informs the thermal stability, including thermal degradation and activation energy, for molding, product handling, and storing along and after service. To the best known of the authors, thermal analysis for acetylated bamboo Betung forming in microfibril cellulose reinforced to PP matrix has not yet been studied. A previous by Jhu *et al.* [11] used bamboo particles then acetylated using acetic anhydride and dimethylformamide solution. Therefore, this research aimed to analyze the effect of acetylated bamboo Betung fiber on the thermal properties of PP biocomposites. The study performs the thermal characteristics of PP biocomposites and the crystallization kinetic under isothermal conditions and isoconversional kinetic on thermal decomposition.

2. Materials and Methods

2.1. Materials

Betung bamboo was obtained from the Bogor Botanical Garden Bamboo Collection. Processing of fibers into pulp was carried out through the kraft process. Betung bamboo pulp was bleached using 50% hydrogen peroxide in technical grade and used as the biocomposite filler. Acetic acid glacial in 99.9% of concentration, 99.9% acetic anhydride, and sulfuric acid in 99.6% of concentration used for acetylation were pure analysis grades obtained from MERCK, Indonesia. Also, homopolymer PP was obtained from PT. Tripolita, Cilegon, Indonesia.

2.2. Acetylated fibers production

According to a previous study by Kusumaningrum *et al.* [3], the acetylation process was conducted. A 5 g of Betung bamboo pulp (dry-based) was activated by using 100 mL of acetic acid for 1 h at room temperature. Furthermore, the acetylation was carried out using 50 mL of acetic anhydride and 2% (w/v) of sulfuric acid. The condition for the process was the temperature at 60°C and 2 h of reaction time. The acetylated fiber was gradually washed using distilled water, ethanol, and acetone until neutral. The acetyl content of acetylated bamboo Betung pulp is 18.19%, and the degree of substitution is 0.83 [3].

2.3. Biocomposites production

Homopolymer PP and Betung bamboo (*D. asper*) fibers were mixed using a Rheomix Haake Polydrive kneader at 180°C for 15 minutes. Fibers were added in 10 and 20% (w/w) for each acetylated and untreated fiber. It was further processed by compression mold using a hot press at 180°C for 2 minutes in 20 MPa. Furthermore, biocomposites were milled into powder form and classified into passed through in 60 and restrained in 100 mesh for DSC (Differential Scanning Calorimetry) analysis and Thermo Gravimetric Analysis. PAB and PBB were used in denoting biocomposites with acetylated and untreated fibers, respectively. The compositions used were 10 and 20% by weight according to the weight of the biocomposite.

2.4. Colorimetric analysis

Color reader CR 1 Konica Minolta was used for colorimetric analysis. Color measurement for biocomposite surfaces and some processes condition that affect the final product's color appearance were recorded. Some spectral classifications were performed using CIELAB coordinates (L^* , a^* , and b^*) according to D65 light source [14]. Five different locations at the biocomposite surface were light shot for each sample. All data were recorded as total color change (ΔE_{ab}) and calculated using the Euclidian distance equation, as shown in Equation 1.

$$\Delta E_{ab} = \sqrt{\Delta L^2 + \Delta a^2 + \Delta b^2} \quad (1)$$

where, ΔL , Δa , and Δb represent the differences between the initial and final product. Each data shows a different light reflection: L value stands for the lightness of the product. A positive Δa denotes a color shift against red

and a negative against green. Positive Δb denotes color shift against yellow and negative against blue.

2.5. Scanning Electron Microscopy (SEM)

SEM Hitachi TM3030 was used for morphological analysis of Betung bamboo pulp before and after acetylation treatment. Samples were coated with gold before analysis. Magnification was carried out at 500× and electron scanning at 5 kV.

2.6. DSC (Differential Calorimetry Analysis)

DSC Perkin Elmer Phyris 1 DSC 4000 equipped with an intercooler was used to investigate the thermal characteristics of the biocomposite. DSC measurement was carried out through several stages. Stage I: sample heating in the calorimeter with a heating rate of 10°C/minute from 30 to 200°C. Stage II: sample was held at 200°C for 5 minutes. Stage III: sample was cooled from 200 to 30°C with a cooling rate of 10°C/minute. The crystallization degree was measured using the ratio between melting fusion enthalpy of biocomposites and pure PP (ΔH_m), which has 100% of the crystallization degree multiplied by the weight fraction of PP biocomposite. The crystallization degree can be measured as shown in Equation 2 [15]. The value of melting enthalpy fusion of pure PP was calculated to be 138 J/g [16].

$$\%X_{cb} = \frac{\Delta H_m}{\Delta H_{mf} W} \quad (2)$$

2.7. Isothermal crystallization kinetics

Crystallization kinetics was performed at isothermal conditions and with the Avrami model approach [17], as shown in Equation 3. Avrami parameters occurred in exothermic conditions. DSC measurement was carried out through the following steps: First, heating 5 mg of samples from 30 to 200°C with a heating rate of 10°C/min. Second, holding at 200°C for 2 minutes, and third, cooling from 200°C aimed to determine its isothermal crystallization temperature (TCs) for 20 minutes with a cooling rate of 40°C/minute.

$$X(t) = 1 - \exp(-\beta t^n) \quad (3)$$

$X(t)$ represents the fraction volume of crystallized biocomposite at a particular t , β was carried out as an Avrami rate constant that reflects crystallization rate. n is an Avrami exponent that shows the crystal geometry. $X(t)$ is a function of time and heat flow in the range of the isothermal crystallization step.

Avrami parameters (β and n) were calculated with a logarithmic equation as represented in Equation 4. Those parameters can be used to calculate the slope for n and intercept for β .

$$\log[-\ln(1 - X(t))] = n \log t + \log \beta \quad (4)$$

2.8. TGA (Thermal Gravimetric Analysis)

TGA was carried out using TGA 4000 Perkin Elmer. 10 mg of biocomposites sample was placed on a ceramic crucible weighing on a furnace holder. TGA analysis was conducted at a heating rate of 10°C/minute from 30 to 600°C.

2.9. Activation Energy

The thermal stability of material can be further explained by using decomposition phenomena. There are many approaches to decomposition reactions. One of the reaction rates is shown in Equation 5.

$$\frac{d\alpha}{dt} = k(T)f(\alpha) \quad (5)$$

where, α is the conversion degree, t is the reaction time, $k(T)$ is the reaction rate constant, and $f(\alpha)$ is the kinetic function. Conversion degree (α) can be defined as the weight reduction ratio, as shown in Equation 6.

$$\alpha = \frac{m_0 - m}{m_0 - m_\infty} \quad (6)$$

where m_0 , m , and m_∞ are the mass 0, t , and termination time, respectively.

The reaction rate constant can be formulated according to the Arrhenius equation, as shown in Equation 7.

$$k(T) = A \exp\left(\frac{-E_a}{RT}\right) \quad (7)$$

where, A is the pre-exponential factor, E_a is the activation energy, T is the absolute temperature, and R is the gas constant.

Equation 8 was formed from Equations (6) and (7) when modified with (5).

$$\frac{d\alpha}{dt} = A \exp\left(\frac{-E_a}{RT}\right) f(\alpha) \quad (8)$$

The activation energy can be determined by the model-free or isoconversional method. Flynn Wall Ozawa (FWO) is one of the accurate models used to carry out decomposition phenomena such as biomass [11] and composite product [12]. These models represent activation energy value on particular conversion, as explained by Koga [18]. Each conversion level can be determined using Equation 9.

$$\ln \gamma = \ln\left(\frac{A\alpha E_a}{Rg(\alpha)}\right) - 5.331 - 1.052\left(\frac{E_a}{RT\alpha}\right) \quad (9)$$

where, $g(\alpha)$ is the constant at a certain conversion level.

The activation energy value can be obtained by plotting the $\ln \gamma$ and absolute temperature, where γ is the heating rate. Also, the activation energy can be obtained using Equation 10.

$$E_a = -\frac{bR}{1.0516} \quad (10)$$

where, b is the slope of the logarithmic curve from the heating rate and absolute maximum temperature for a given conversion level.

3. Results and Discussion

3.1. Colorimetric analysis of product

The mixing process used rheomix laboplastomill to disperse and mix the fibers into a PP matrix. Therefore, the mixing condition was set at 180°C, which exceeded the melting point of PP. This process was carried out to evenly distribute the fiber onto the matrix on the melting polymer. This produced biocomposite with different

appearances for untreated and acetylated fibers addition. The chemical composition of fibers affects these features.

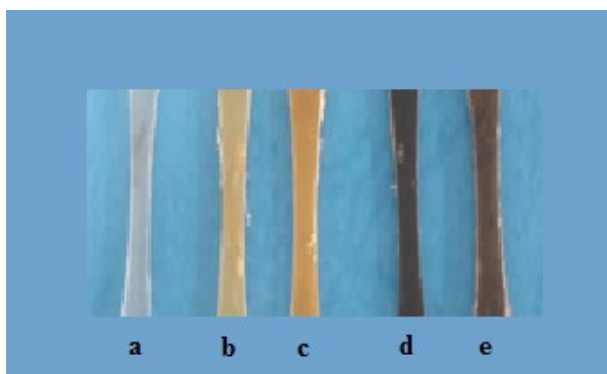


Figure 1. The appearance of pure PP (a), biocomposite with untreated fiber PBB 10 (b), PBB 20 (c), biocomposites with acetylated fiber PAB 10 (d), PAB 20 (e)

Furthermore, the mixing process that uses laboplastomill causes the fibers to be well dispersed on the matrix. High fiber loading gives darker color for untreated and acetylated fibers biocomposites, as shown in Figure 1, due to the heating process on composites mixing that further affects the thermal decomposition of original fibers in white color both for untreated and acetylated fibers, as shown in Figure 2. In composite without heating process, such as polyvinyl alcohol and fibers composites, the color of composites are naturally similar to fiber color [19]. The total color change (ΔE_{ab}) also shows the color differences between PP and biocomposite, as shown in Table 1. Biocomposite is darker than PP due to its lower L value, indicated by the negative result, and ΔL , which indicates a total change in lightness, is decreasing. The PAB biocomposite is darker than PBB. The total color change was known by its lightness and chromaticity coordinates due to greater change between PP and biocomposite. The pulp that has been treated with the acetylation process is partially carbonized during the mixing process.

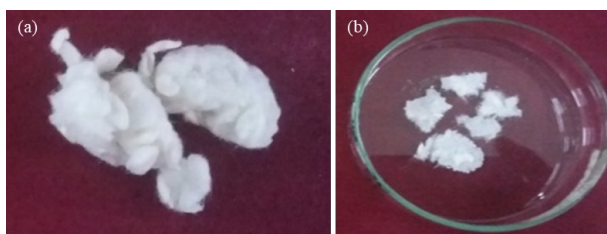


Figure 2. The appearance of Betung bamboo pulp without treatment (a) and with acetylation (b)

Table 1. Color change of PP and biocomposites product

°	L	A	b	ΔL	Δa	Δb	ΔE_{ab}
PP	46.98	9.84	17.34				
PBB 10	45.58	10.88	21.04	-1.4	1.04	3.7	4.09
PBB 20	43.5	12.98	20.7	-3.48	3.14	3.36	5.77
PAB 10	28.78	8.96	8.54	-18.2	-0.88	-8.8	20.23
PAB 20	24.9	6.12	9.42	-22.08	-3.72	-7.92	23.75

The decomposition of untreated and acetylated fiber is shown in Figure 3. Acetylated fiber started to

decompose at 238.15°C, lower than untreated fiber, which decomposed at 322.93°C. A decomposition temperature close to the mixing temperature, at 180°C, caused some of the acetylated fibers to decompose, thus producing biocomposite with a darker color. Untreated fiber has three stages of decomposition temperature: Stage 1 occurs at 30–240°C with a temperature peak at 68.62°C where water evaporation occurs. Stage 2 occurs at 250–360°C, where the crystalline part of cellulose rapidly decomposes, while Stage 3 occurs at 360–500°C, where decomposition of the amorphous part occurs. Acetylated fiber also has three stages of decomposition temperatures. The first stage occurs at 30–200°C, corresponding to water evaporation and loss of weight. This shows that acetylated fiber is more hydrophobic than untreated fibers and allows limited water absorption, so bounded water content could be lower than untreated fibers. The reduction of moisture uptake in the decomposition stage of less than 100°C indicates the reduction of hydrophilic properties of acetylated fibers [5]. It might happen due to substituting the acetyl group for the hydroxyl groups in the fiber surface [20]. The second stage occurs at 200–365°C, representing the crystalline part decomposition. While the third stage, which occurs at 365–500°C, shows amorphous part decomposition. According to Ashori *et al.* [21], acetylation enhanced kenaf fiber’s decomposition temperature with 10.5% acetyl content.

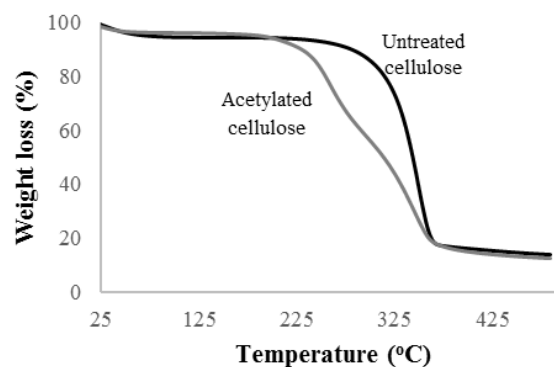


Figure 3. TGA thermogram of untreated and acetylated fiber from Betung bamboo

Furthermore, lower decomposition temperature resulted in acetyl content with more value than that. In this case, acetylated fibers from Betung bamboo with 18.19% of acetyl content might affect lower decomposition temperature than untreated fibers due to higher acetyl content, more than 10.5%. According to Chung *et al.* [22], the higher degree of substitution correlated higher with acetyl content, which would increase the fiber’s roughness due to the modification mechanism by strong acids to substitute the hydroxyl groups for acetyl groups. The fiber surface of acetylated fiber appeared rougher surface and smaller diameter than untreated fiber, as shown in Figure 4, contributing to hydroxyl group exposure from cellulose. Disruption of hydrogen bonding in cellulose structure increases fiber surface roughness and removes the amorphous part in the fiber cell wall allowing for smaller diameters of acetylated fiber [6]. Sulfuric acid in the acetylation solution may degrade cellulose attributed to rougher and

smaller fiber than untreated fiber causing low decomposition temperature [23, 24]. Nevertheless, rougher fiber surfaces facilitate interlocking and nucleating growth between fiber and matrix to improve the mechanical and thermal properties of composites.

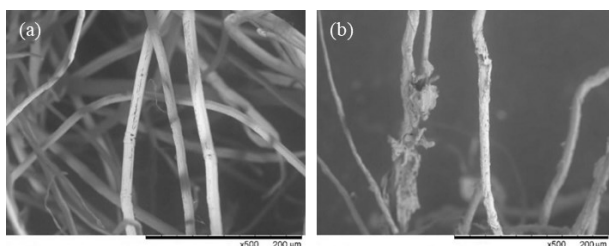


Figure 4. SEM characterization of Betung bamboo (*D. asper*) pulp before treatment (a) and with acetylation (b)

3.2. Differential Calorimetry (DSC): Thermal characteristics and crystallization kinetic

Fiber treatment as a reinforcing agent for biocomposites has different effects. Other than mechanical properties, this treatment also affects thermal properties. Figure 5 and 6 represents the DSC analysis of biocomposite with untreated and acetylated fibers in endothermic and exothermic conditions. The melting temperature of biocomposite products is similar to pure PP, which ranges from 161 to 162°C, while the melting point for PP is 162.16°C. The addition of 20% fiber does not make a significant enhancement both for PBB and PAB. This marginal result shows that a non-reversible reaction occurred on the endothermic step. It further explains that PP, PAB, and PBB undergo complete melting for each stack of lamella [9].

Meanwhile, PAB shows melting point and melting fusion lower than PP, even at a minor point. This corresponds to lower melting energy of biocomposite than pure PP [7]. Luz *et al.* [15] reported that the biocomposite's melting point and melting fusion from PP and bagasse fiber were reduced after acetylation treatment. This shows that there is some interaction between microfibril cellulose and PP.

Crystallization degrees for PBB and PAB biocomposites are shown in Table 2. Fibers, in addition to PP, enhanced crystallization degree compared to pure PP. Fibers with 20% composition improved the crystallization degree for both PBB and PAB. PAB biocomposite also has more favorable results than PBB. This shows fibers as a nucleating agent in the crystallization process for biocomposite, and acetylated fibers provide better nucleating ability than untreated ones.

The exothermic condition represents crystallization temperature, as shown in Figure 6. Biocomposite of acetylated and untreated fibers have high crystallization temperatures than pure PP. Fiber loading up to 20% improves crystallization temperature for PAB biocomposite. Meanwhile, the enhancement does not occur for PBB, as shown in Table 2. The enhancement of crystallization temperature on PAB, including fiber addition, shows that acetylated fibers initiate nucleation and accelerate the crystallization process of biocomposite

[8] and provide a large surface area for the crystals to grow [25]. In addition, this was due to better macromolecular reorganization of amorphous into crystalline parts of biocomposite than pure PP [7].

Crystallization of biocomposite is a solidification process influenced by several factors such as crystallization temperature, cooling rate, and nucleating agent effectivity. These factors affect the crystal growth rate. Isothermal crystallization can be determined at a specific crystallization temperature with a fast cooling rate. Furthermore, the Avrami model identifies crystallization growth rate constants. Assumptions made for this model are that crystal growth starts to develop along the fiber surface and randomly grows in all directions. This research determined isothermal crystallization temperatures at 123, 127, and 132°C with a fast cooling rate of 40°C/minute. Papageorgiou *et al.* [26] reported that several factors influenced the biocomposite properties of polyolefin polymer: filler content, morphology, time and temperature process, crystallinity, and crystallization rate during solidification from the melting phase.

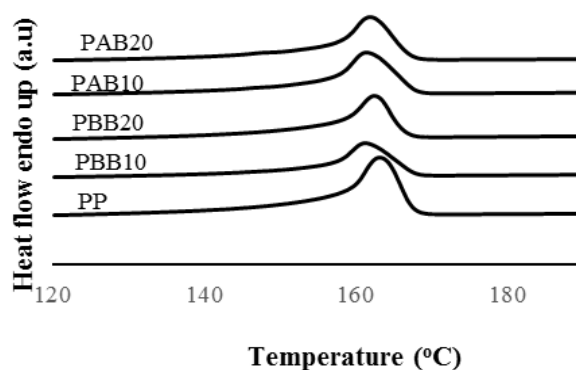


Figure 5. DSC endothermic thermogram of biocomposites

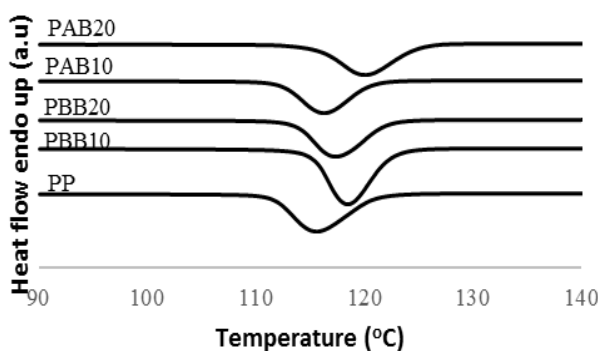


Figure 6. DSC exothermic thermogram of biocomposites

Polymer crystallization consists of two steps: primary and secondary crystallization. Primary crystallization is related to the nucleus and crystal growth up to the edge of the spherulites and crashes the adjacent spherulite edge. The filler characteristic strongly affects the primary crystallization because it occurs quickly. Secondary crystallization, in which crystal growth occurs between formed spherulites, is slower than primary. Avrami parameters (n and β) show the entire

crystallization process, including nucleation and crystal growth. Table 3 shows the Avrami parameters for biocomposite. n value represents nucleation mechanism and crystal morphology or geometry. Avrami [17] and Avrami [27] explained that the n value is an integer number ranging from 1 to 4. The value between 1 and 3 represents heterogeneous nucleation, while above 3 is homogeneous. n value for all biocomposites ranging from 1.9 to 3 indicates that the solidification process on PBB and PAB is heterogeneous nucleation.

Table 2. Thermal properties and crystallization degree of biocomposites

Biocomposite	First heating		Cooling		Second heating		%X _{cb}
	T _m (°C)	ΔH _m (J/g)	T _c (°C)	ΔH _c (J/g)	T _m (°C)	ΔH _m (J/g)	
PP	163.66	76.79	115.52	72.93	162.16	79.24	57.41
PBB 10	163.5	77.96	119.12	80.64	161.67	71.80	57.80
PBB 20	163.53	60.04	117.35	72.76	162.37	67.75	61.37
PAB 10	163.69	70.20	117.74	83.25	161.36	73.90	59.50
PAB 20	163.36	70.98	120.13	65.94	161.87	72.15	65.35

Meanwhile, the geometry of the crystal formed is spherulite. Heterogeneous nucleation occurs when spherulite crystals randomly grow along the fiber surface, and form impeded nucleus on the polymer matrix [11]. According to Abadchi and Jalali-Arani [28], the n value is related to the crystal dimension. It is proportional to the dimension or formed crystal radius.

Another Avrami parameter, β value, is correlated to the nucleation process and crystal growth rate. It is inversely proportional to isothermal crystallization temperature, as shown in Table 3. Several types of the research reported that isothermal crystallization rate and temperature are inversely proportional [28, 29] due to lower nucleating ability effectiveness at higher isothermal crystallization temperature because the nucleus number is inversely proportional to the temperature, which takes a longer solidification process [11, 30]. Furthermore, Jhu *et al.* [11] explained that high T_m and T_cs differences increase the nucleus density at the fiber surface, leading to faster and more nucleus growth. PAB shows high β value than PP and PBB. The β value increased by 2.6 up to 4.5-fold in 10% and 20% of acetylated fiber loading than PP in high isothermal crystallization temperature, respectively. It emphasized that acetylated fiber acts as the nucleating agent, increasing the PAB’s crystallization rate. The additional fibers also increase the β value for both PAB and PBB. In this research, acetylated and untreated fiber can act as nucleating agents, but the impact will be relatively different. Jhu *et al.* [9] confirmed that trans-crystallization and compatibilities of PP matrix with unmodified and acetylated fibers affect crystallization, including crystallization rate and mechanism.

Furthermore, lower acetyl content promotes heterogeneous nucleation, high nucleus density, and trans-crystallization in the PP matrix than higher acetyl

content which has lower nucleus density and promotes homogeneous nucleation [11]. Beta phase formation of PP biocomposites indicated trans-crystallization phenomena on the fiber surface, which correlated to mechanical properties enhancement than pure PP [3]. Acetylated fiber facilitates nucleating ability with heterogenous nucleation mechanism on PP matrix corresponding to the enhancement of crystallization temperature and crystallization degree as well as crystallization rate of PAB biocomposites.

Table 3. Avrami parameters for isothermal crystallization kinetics of biocomposites

Biocomposite	Crystallization Temperature (°C)	β min ⁻¹	n
PP	123	0.848	2.62
	127	0.138	
	132	0.010	
PBB 10	123	0.184	2.79
	127	0.051	
	132	0.001	
PBB 20	123	0.502	2.53
	127	0.143	
	132	0.005	
PAB 10	123	1.089	2.67
	127	0.214	
	132	0.026	
PAB 20	123	1.215	1.97
	127	0.656	
	132	0.045	

3.3. Thermogravimetric analysis (TGA) and activation energy of biocomposites product

TGA analysis shows the decomposition temperature of the biocomposite compared to PP, as shown in Figure 7. The T_{onset} is the initial temperature when the biocomposite starts to decompose. PP has one decomposition stage while PBB and PAB biocomposite has two, which shows different decomposition temperatures for each component and is lower for biocomposite than PP. Meanwhile, PBB has a lower decomposition temperature than PAB, especially on 10% fiber addition. After 20% of fiber addition, it shows a lower decomposition temperature for both PAB and PBB. Biocomposites PAB 20 has the lowest T_{onset}, which is about 311.25°C only in the first decomposition stage, contrary to PAB 10, which has the highest T_{onset}, about 366.7°C, than PBB, as shown in Table 4. TGA analysis was carried out for biocomposite after mixing, leading to fibers’ carbonization. However, with 20% fiber, some remains an acetylated fiber. This is due to the lower decomposition of acetylated fiber than untreated fiber, as shown in Figure 4. Meanwhile, in the second decomposition stage, the T_{onset} of biocomposite PAB 10 and PAB 20 is 375–500°C and increased from 3–6°C to PP. This result further shows that acetylated fiber affects the thermal stability of biocomposite even with slight differences.

Table 4. Thermal characteristic of PP and biocomposites by TGA/DTG

Biocomposite	T_{onset} (°C)	T_{max} (°C)	m_{max} (mg/min)	Char residue at 550°C (%)		
PP	440.16	467.01	0.16	0.01		
PBB 10	341.94	441.96	349.74	467.24	0.19	0.83
PBB 20	325.04	442.38	351.67	467.74	0.16	1.33
PAB 10	366.7	443.37	379.08	465.66	0.16	0.14
PAB 20	311.25	446.45	347.97	469.98	0.17	2.26

The single decomposition peak is reported for PP, while two peaks for biocomposites PBB and PAB are shown in Figure 8. T_{max} was the decomposition temperature when the maximum weight loss rate occurred. The decomposition temperature of pure PP occurred at 467°C and rapidly rose to 500°C. The first decomposition temperature for biocomposite ranges from 200°C to 375°C, as shown in Figure 8, and the second temperature ranges from 400°C to 550°C. This result confirms that carbon atomic decomposition is higher than fibers. The thermal stability of PP is affected by branching, where the carbon atomic of PP is mainly a tertiary carbon which is more difficult to degrade [31].

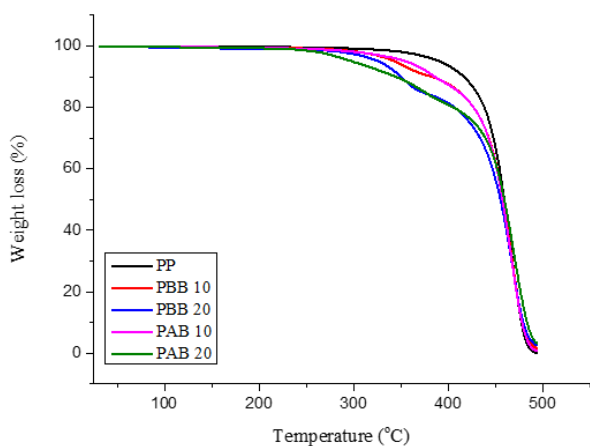


Figure 7. TGA analysis of biocomposites

Furthermore, the T_{max} of PBB biocomposite is lower than PAB at first up to 10% of fiber addition, as shown in Table 4. This result shows that carbonized acetylated fiber remains heat resistant; therefore, maximum weight loss occurs at high temperatures. The decomposition temperature of carbonized basalt fiber on PP composites increases by about 5–10°C after 10–50% of weight loss, corresponding to the thermal stability of carbonized fibers at higher temperatures [32]. Second decomposition

temperature, which is similar to the breakdown of the PP chain, the PBB biocomposite is similar to pure PP. Meanwhile, this is different for PAB biocomposites, especially for PAB 20, which maximum decomposition temperature has a higher value than pure PP. High molecular weight occurs from cross-linking reaction between acetylated fiber and PP matrix, resulting in higher decomposition temperature in the last stage [7].

Furthermore, char residue from PAB 20 has a higher value than others. High char residue shows the improvement of thermal stability of HDPE composites filled with wood flour even with slight difference [20]. Carbon fiber on PP composites increases the char content due to its good barrier ability to thermal degradation, which slows down the weight loss rate of PP composites decomposition [33], which means PAB is more thermally stable than pure PP and PBB.

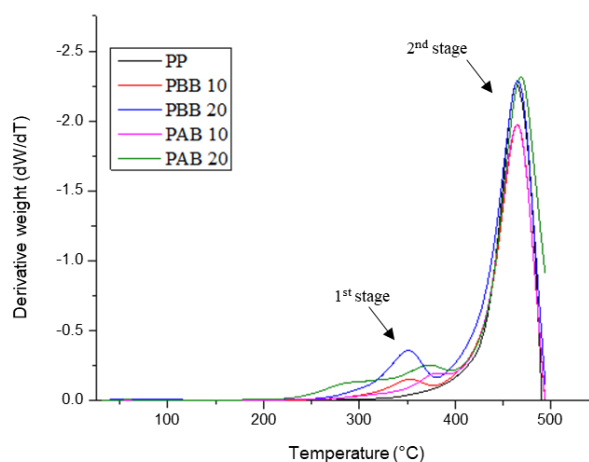


Figure 8. DTG analysis of biocomposites

The FWO-free model allows activation energy for certain conversion levels. Heating rates used for this measurement are 5, 10, and 15°C/minute. Table 5 shows the activation energy for pure PP and biocomposite on conversion levels 0.1–0.9. According to the result, the activation energy of biocomposite has two maximum levels at conversion, 0.1 and 0.9, whereas PP only has one at 0.9. According to the DTG data shown in Figure 8, the decomposition of biocomposite occurred at 10% and 90% of weight loss. This shows that decomposition is proportional to the maximum activation energy. The average activation energy for PP is slightly higher than for the biocomposite. The decomposition activation energy of PP is about 14,0–176 kJ/mol. The lower activation energy of a low conversion level is due to degradation side chain scission, which increases as the conversion level increases due to the decomposition of random chain scission forming various monomers and oligomers [31]. The activation energy of biocomposites is relatively higher than PP at a low conversion level because of the complex structure combining interfacial bonding between PP and fibers. This higher initial decomposition allows for thermally stable biocomposites.

Table 5. The activation energy of biocomposites through the FWO model

α	PP		PBB 10		PBB 20		PAB 10		PAB 20	
	Ea (kJ/mol)	R ²	Ea (kJ/mol)	R ²	Ea (kJ/mol)	R ²	Ea (kJ/mol)	R ²	Ea (kJ/mol)	R ²
0.1	139.52	0.96	310.87	0.93	173.76	0.89	209.46	0.84	226.99	0.97
0.2	170.86	0.99	238.17	0.98	130.03	0.86	117.35	0.82	170.51	0.98
0.3	191.25	0.99	252.66	0.99	144.48	0.88	130.72	0.86	139.85	0.95
0.4	203.22	0.99	265.19	0.99	152.49	0.89	145.87	0.88	152.39	0.95
0.5	210.20	0.99	271.36	0.99	157.68	0.90	156.31	0.90	160.91	0.95
0.6	215.52	0.99	276.66	0.99	162.14	0.91	163.83	0.90	167.68	0.95
0.7	221.53	0.99	280.14	0.99	166.53	0.92	170.26	0.91	174.95	0.95
0.8	227.92	0.99	279.17	0.99	171.18	0.92	177.27	0.92	181.75	0.95
0.9	233.30	0.99	286.76	0.99	178.17	0.93	185.32	0.92	193.07	0.95
Mean	201.48		273.44		159.61		161.82		174.23	

Furthermore, the addition of 20% fibers to PAB improved the activation energy. Meanwhile, it lowers the activation energy of PBB. In addition, it can be deduced that the acetylation process of fibers improves the thermal stability of the biocomposite. The calculated squares of the correlation coefficient, R², ranged from 0.93 to 0.99, 10 and 20 for PP, PBB and PAB biocomposites respectively. Different results were obtained for PAB 10 and PBB 20, ranging from 0.82 to 0.92. This can be analyzed further by another model and can be described with a different mechanism. Also, the conversion level is proportional to R² for all biocomposites. This shows that the first order of decomposition kinetics only applies at a high conversion level, where R² is more than 90%, as confirmed by Guo *et al.* [25]. Furthermore, it shows that the first-order kinetic PP model only applies at a conversion level of 0.7–0.9. The random scission of fibers decomposition, detected at a low conversion level, cannot be explained by the first-order kinetics model.

4. Conclusion

This research investigated the effects of the acetylation of Betung bamboo pulp on the thermal characteristics of PP biocomposites. It was seen that the surface roughness of bamboo pulp increased by acetylation, with an onset temperature reduction of around 20% than untreated fiber. The darker appearance of biocomposite with acetylated fibers confirmed that some fibers underwent carbonization during mixing. Furthermore, according to DSC and TGA analysis, the acetylation process on the Betung bamboo pulp surface made it more thermally stable on PP biocomposite. The DSC analysis showed that acetylated fiber improved crystallization temperature and degree by adding 20% fiber to PP. Crystallization kinetic study using the Avrami model showed that acetylated fiber accelerates the nucleating and crystal growing process up to 4.5-fold more than PP in spherulitic crystal form by heterogeneous nucleation mechanism. TGA analysis for two decomposition stages of biocomposite showed that onset and maximum decomposition temperature improved after adding acetylated fibers up to 10%. However, the maximum decomposition temperature

improved, especially in the second stage, after adding up to 20% acetylated fibers. The activation energy of biocomposite had two maximum values at conversion levels of 0.1 and 0.9, which indicate maximum decomposition energy at 10 and 90% of weight loss. Generally finding, the role of acetylated Betung bamboo fiber is as a nucleating agent in the PP matrix and moderately improving the maximum thermal decomposition of biocomposites. This result provides information about the manufacturing process and after-service treatment of biocomposites.

Acknowledgment

The authors thank the Ministry of Research, Technology and Higher Education, Indonesia, for funding this research to the thematic program Laboratory of Biocomposite Engineering and Ecostructure, the Research Center for Biomaterials, and the National Research and Innovation Agency for their support.

References

- [1] Hisham A. Maddah, Polypropylene as a promising plastic: A review, *American Journal of Polymer Science*, 6, 1, (2016), 1–11
- [2] Fernando Rusch, Arci Dirceu Wastowski, Taisa Shimosakai de Lira, Kelly Costa Cabral Salazar Ramos Moreira, Danielle de Moraes Lucio, Description of the component properties of species of bamboo: a review, *Biomass Conversion and Biorefinery*, 13, (2023), 2487–2495 <https://doi.org/10.1007/s13399-021-01359-3>
- [3] Wida Banar Kusumaningrum, R. Rochmadi, S. Subyakto, Pembuatan Selulosa Terasetilasi dari Pulp Bambu Betung (*Dendrocalamus asper*) serta Pengaruhnya Terhadap Sifat Mekanis Biokomposit Polipropilena, *Reaktor*, 17, 1, (2017), 25–35 <https://doi.org/10.14710/reaktor.17.1.25-35>
- [4] Lang Huang, Qiong Wu, Shujun Li, Rongxian Ou, Qingwen Wang, Toughness and crystallization enhancement in wood fiber-reinforced polypropylene composite through controlling matrix nucleation, *Journal of Materials Science*, 53, (2018), 6542–6551 <https://doi.org/10.1007/s10853-018-1996-y>

- [5] Hamideh Hajiha, Mohini Sain, Lucia H. Mei, Modification and characterization of hemp and sisal fibers, *Journal of Natural Fibers*, 11, 2, (2014), 144-168 <https://doi.org/10.1080/15440478.2013.861779>
- [6] Taimur-Al-Mobarak, M. F. Mina, M. A. Gafur, A. N. Ahmed, S. A. Dhar, Effect of chemical modifications on surface morphological, structural, mechanical, and thermal properties of sponge-gourd natural fiber, *Fibers and Polymers*, 19, (2018), 31-40 <https://doi.org/10.1007/s12221-018-7199-3>
- [7] Haydar U. Zaman, Ruhul A. Khan, Acetylation used for natural fiber/polymer composites, *Journal of Thermoplastic Composite Materials*, 34, 1, (2021), 3-23 <https://doi.org/10.1177/0892705719838000>
- [8] Jaegwan Moon, Jong Hoon Lee, Kiseob Gwak, Wanhee Im, Characteristics of polypropylene biocomposites: effect of chemical treatment to produce cellulose microparticle, *Cellulose*, 29, 12, (2022), 6733-6743 <https://doi.org/10.1007/s10570-022-04691-7>
- [9] Yu-Shan Jhu, Teng-Chun Yang, Ke-Chang Hung, Jin-Wei Xu, Tung-Lin Wu, Jyh-Horng Wu, Nonisothermal crystallization kinetics of acetylated bamboo fiber-reinforced polypropylene composites, *Polymers*, 11, 6, (2019), 1078 <https://doi.org/10.3390/polym11061078>
- [10] Sung-Hoon Kim, Eui-Su Kim, Kisuk Choi, Jung Keun Cho, Hanna Sun, Ji Wang Yoo, In-Kyung Park, Youngkwan Lee, Hyouk Ryeol Choi, Taesung Kim, Rheological and mechanical properties of polypropylene composites containing microfibrillated cellulose (MFC) with improved compatibility through surface silylation, *Cellulose*, 26, (2019), 1085-1097 <https://doi.org/10.1007/s10570-018-2122-7>
- [11] Yu-Shan Jhu, Ke-Chang Hung, Jin-Wei Xu, Tung-Lin Wu, Jyh-Horng Wu, Transcrystallization of the acetylated bamboo fiber/polypropylene composite under isothermal crystallization, *Wood Science and Technology*, 55, (2021), 797-810 <https://doi.org/10.1007/s00226-021-01279-5>
- [12] Noura Hamour, Amar Boukerrou, Alain Bourmaud, Hocine Djidjelli, Yves Grohens, Effect of alfa fiber treatment and MAPP compatibilization on thermal and mechanical properties of polypropylene/alfa fiber composites, *Cellulose Chemistry and Technology*, 50, 9-10, (2016), 1069-1076
- [13] Noura Hamour, Amar Boukerrou, Hocine Djidjelli, Jean-Eudes Maigret, Johnny Beaugrand, Effects of MAPP compatibilization and acetylation treatment followed by hydrothermal aging on polypropylene alfa fiber composites, *International Journal of Polymer Science*, 2015, 451691, (2015), <https://doi.org/10.1155/2015/451691>
- [14] Yao Chen, Nicole M. Stark, Mandla A. Tshabalala, Jianmin Gao, Yongming Fan, Weathering characteristics of wood plastic composites reinforced with extracted or delignified wood flour, *Materials*, 9, 8, (2016), 610 <https://doi.org/10.3390/ma9080610>
- [15] S. M. Luz, J. Del Tio, G. J. M. Rocha, A. R. Gonçalves, A. P. Del'Arco Jr, Cellulose and cellulignin from sugarcane bagasse reinforced polypropylene composites: Effect of acetylation on mechanical and thermal properties, *Composites Part A: Applied Science and Manufacturing*, 39, 9, (2008), 1362-1369 <https://doi.org/10.1016/j.compositesa.2008.04.014>
- [16] P. V. Joseph, K. Joseph, Sabu Thomas, C. K. S. Pillai, V. S. Prasad, Gabriël Groeninckx, Mariana Sarkissova, The thermal and crystallisation studies of short sisal fibre reinforced polypropylene composites, *Composites Part A: Applied Science and Manufacturing*, 34, 3, (2003), 253-266 [https://doi.org/10.1016/S1359-835X\(02\)00185-9](https://doi.org/10.1016/S1359-835X(02)00185-9)
- [17] Melvin Avrami, Kinetics of phase change. I General theory, *The Journal of Chemical Physics*, 7, (1939), 1103-1112 <https://doi.org/10.1063/1.1750380>
- [18] Nobuyoshi Koga, Ozawa's kinetic method for analyzing thermoanalytical curves: History and theoretical fundamentals, *Journal of Thermal Analysis and Calorimetry*, 113, (2013), 1527-1541 <https://doi.org/10.1007/s10973-012-2882-5>
- [19] K. W. Prasetyo, W. B. Kusumaningrum, Properties of polyvinyl alcohol composite filled Ampel bamboo (*Bambusa vulgaris*) microfibrils fibrillated by mechanical treatment, *IOP Conference Series: Earth and Environmental Science*, 2020 <https://doi.org/10.1088/1755-1315/572/1/012042>
- [20] R. F. Buson, L. F. L. Melo, M. N. Oliveira, G. A. V. P. Rangel, E. P. Deus, Physical and mechanical characterization of surface treated bamboo fibers, *Science and Technology of Materials*, 30, 2, (2018), 67-73 <https://doi.org/10.1016/j.stmat.2018.03.002>
- [21] Alireza Ashori, Mehran Babaee, Mehdi Jonoobi, Yahya Hamzeh, Solvent-free acetylation of cellulose nanofibers for improving compatibility and dispersion, *Carbohydrate Polymers*, 102, (2014), 369-375 <https://doi.org/10.1016/j.carbpol.2013.11.067>
- [22] Taek-Jun Chung, Ji-Won Park, Hyun-Ji Lee, Hueck-Jin Kwon, Hyun-Joong Kim, Young-Kyu Lee, William Tai Yin Tze, The improvement of mechanical properties, thermal stability, and water absorption resistance of an eco-friendly PLA/kenaf biocomposite using acetylation, *Applied Sciences*, 8, 3, (2018), 376 <https://doi.org/10.3390/app8030376>
- [23] Adane Dagnaw Gudayu, Leif Steuernagel, Dieter Meiners, Rotich Gideon, Effect of surface treatment on moisture absorption, thermal, and mechanical properties of sisal fiber, *Journal of Industrial Textiles*, 51, 2_suppl, (2022), 2853S-2873S <https://doi.org/10.1177/1528083720924774>
- [24] Thiago Souza Da Rosa, Rosilani Trianoski, Franck Michaud, Christophe Belloncle, Setsuo Iwakiri, Efficiency of different acetylation methods applied to cellulose fibers waste from pulp and paper mill sludge, *Journal of Natural Fibers*, 19, 1, (2022), 185-198 <https://doi.org/10.1080/15440478.2020.1731909>
- [25] Lei Guo, Fengxiang Chen, Yingshan Zhou, Xin Liu, Weilin Xu, The influence of interface and thermal conductivity of filler on the nonisothermal crystallization kinetics of polypropylene/natural protein fiber composites, *Composites Part B: Engineering*, 68, (2015), 300-309 <https://doi.org/10.1016/j.compositesb.2014.09.004>
- [26] Dimitrios G. Papageorgiou, Konstantinos Chrissafis, Dimitrios N. Bikiaris, β -nucleated polypropylene: processing, properties and nanocomposites, *Polymer Reviews*, 55, 4, (2015), 596-629 <https://doi.org/10.1080/15583724.2015.1019136>

- [27] Melvin Avrami, Kinetics of phase change. II transformation-time relations for random distribution of nuclei, *The Journal of Chemical Physics*, 8, 2, (1940), 212-224
<https://doi.org/10.1063/1.1750631>
- [28] Majid Rezaei Abadchi, Azam Jalali-Arani, Crystallization and melting behavior of polypropylene (PP) in (vulcanized nanoscale polybutadiene rubber powder/PP) polymer-nanocomposites, *Thermochimica Acta*, 617, (2015), 120-128 <https://doi.org/10.1016/j.tca.2015.08.027>
- [29] Vahid Khoshkava, Hesam Ghasemi, Musa R. Kamal, Effect of cellulose nanocrystals (CNC) on isothermal crystallization kinetics of polypropylene, *Thermochimica Acta*, 608, (2015), 30-39
<https://doi.org/10.1016/j.tca.2015.04.007>
- [30] Chunjiang Xu, Qaolian Lv, Defeng Wu, Zhifeng Wang, Polylactide/cellulose nanocrystal composites: a comparative study on cold and melt crystallization, *Cellulose*, 24, (2017), 2163-2175
<https://doi.org/10.1007/s10570-017-1233-x>
- [31] Pallab Das, Pankaj Tiwari, Thermal degradation kinetics of plastics and model selection, *Thermochimica Acta*, 654, (2017), 191-202
<https://doi.org/10.1016/j.tca.2017.06.001>
- [32] Chunhong Tang, FengXiang Xu, Guangyao Li, Combustion performance and thermal stability of basalt fiber-reinforced polypropylene composites, *Polymers*, 11, 11, (2019), 1826
<https://doi.org/10.3390/polym11111826>
- [33] Djamila Kada, Ahmed Koubaa, Ghezalla Tabak, Sebastien Migneault, Bertrand Garnier, Abderrahim Boudenne, Tensile properties, thermal conductivity, and thermal stability of short carbon fiber reinforced polypropylene composites, *Polymer Composites*, 39, S2, (2018), E664-E670
<https://doi.org/10.1002/pc.24093>